1-4

歯周組織破壊とサイトカイン

病変の進行と免疫応答

プラークの侵襲により歯肉炎が発症し、時間の経過とプラーク細菌の質的量的変化にともなって病理組織像は劇的に変化していくが、そのすべての過程でさまざまなサイトカインと呼ばれるタンパク質が関与している（表4、図4）。

①歯肉軟組織の変化（歯肉炎の成立）

臨床的に健康な歯周組織をもつ成人であっても、多形核白血球の歯肉溝への浸潤が観察される。これはプラーク細菌由来のFMLPや細菌抗原刺激により歯肉上皮細胞から産生されるIL-8により生じる。プラークの蓄積は上皮細胞によるさらに大量の炎症性メディエーターの産生を誘導し、それらが結合組織に到達して血管に作用すると、透過性の亢進を引き起こす。さらに炎症性サイトカインの作用を受けた血管内皮細胞は細胞接着分子の発現やmonocyte chemoattractant protein -1(MCP-1)の産生を介して持続的な多形核白血球の浸潤・遊走を誘導し、さらに単球やリンパ球の血管外への遊走を引き起こす。走化性因子の濃度勾配により多形核白血球は歯肉溝に至り、そこで貪食・殺菌を行って歯肉溝から細菌を除去する。しかし、大量の細菌を貪食した多形核白血球は自壊し、放出された酵素は組織に傷害を与える。

②歯肉炎から歯周炎へ

プラークの刺激がさらに持続すると、血管から結合組織に浸潤してくる細胞は主としてT細胞になる。歯肉炎組織中のT細胞のほとんどはCD4陽性、CD45RO陽性のメモリータイプである。マクロファージによって活性化されたT細胞は種々のサイトカイン（IL-2、IL-4、IL-5、IL-6、IL-10、IL-13、IFN-γ）などを産生する。T細胞の産生するIFN-γはマクロファージや線維芽細胞を活性化し、炎症性サイトカインの産生や細胞接着分子の発現を誘導し、炎症反応を修飾する。炎症の持続は接合上皮の傷害と上皮の根尖側への増殖を誘導することになり、歯肉溝は深化する。歯肉溝内の環境の変化は細菌叢の変化を誘発することになり、グラム陰性細菌の増殖、結合組織固有層におけるコラーゲン線維の破壊とB細胞・形質細胞主体の病変へと移行する。B細胞はT細胞による抗原特異的な活性化およびLPSによる多クローン性の活性化をうけて、抗体産生が増強される。その結果、いわゆるB細胞病変と呼ばれる組織像を呈すようになる。

③確立期病変の成立

B細胞病変中ではさまざまな自己反応性のT細胞・B細胞も見られるようになる。これらは自己組織の傷害あるいは変性自己組織の排除にはたらいていると考えられる。また、自己反応性T細胞の増加にともなって、種々の制御性T細胞サブセットも増加してくる。局所では炎症性サイトカイン産生の増加とともに、IL-10、TGF-βといった抑制性サイトカインの産生も増強される。その結果、細胞間相互作用はより複雑な様相を呈するようになる。歯槽骨近傍ではIL-1、TNF-α、RANKLなどの作用により破骨細胞が活性化され、歯槽骨吸収が生じる。組織像は基本的にはB細胞病変であるが、歯周ポケットの形成も生じ、プラーク細菌の持続的な作用により、ポケット上皮内あるいは直下結合組織には好中球、マクロファージも検出される[20]。

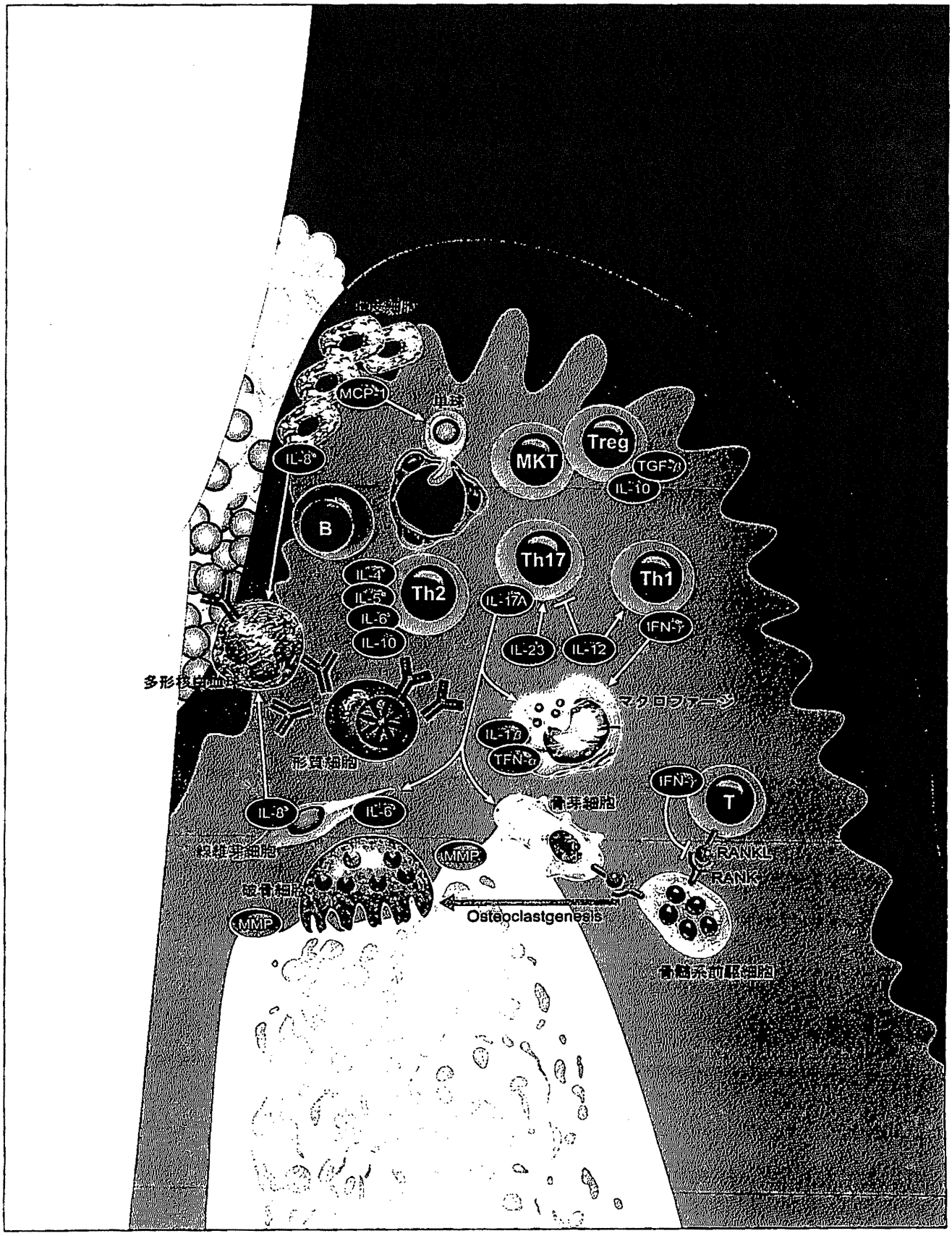

図4　歯周炎組織における免疫応答。

歯周炎組織中ではさまざまな自然免疫、適応免疫の担当細胞が、サイトカインを代表とする液性因子や細胞膜上に発現する分子を介した細胞間接触により相互に制御し、感染防御機構を担っている。同時に、炎症性サイトカインはMMPなどのタンパク分解酵素産生を促進させ、RANKLによる破骨細胞の分化・活性化と強調して、結合組織破壊や歯槽骨吸収といった歯周炎に特徴的な病態の形成に関与している。

表4　歯周組織にみられる代表的サイトカイン。

	主要な産生細胞	主要な標的細胞	作用・その他
IL-1	単　球 マクロファージ	上皮細胞 線維芽細胞 T/B 細胞 破骨細胞 血管内皮細胞	IL-8 や MCP-1 などのケモカインの産生亢進 IL-6 や IL-8 などの産生，MMP，PGE_2 の産生増強 サイトカイン産生 破骨細胞の活性化 ケモカイン産生
IL-2	T 細胞	T 細胞 B 細胞 NK 細胞	細胞増殖，サイトカイン産生誘導 細胞増殖，抗体産生誘導 細胞増殖，活性化
IL-4	T 細胞 (Th2) 肥満細胞 NKT 細胞	B 細胞 T 細胞 血管内皮細胞	MHC Class II 発現誘導，IgE の産生 Th1 の抑制 接着分子 VCAM-1 の発現誘導によるリンパ球の血管接着促進
IL-6	単　球 マクロファージ T/B 細胞 血管内皮細胞 線維芽細胞 脂肪細胞	T/B 細胞 血管内皮細胞 肝細胞	B 細胞増殖・分化を誘導 接着分子 VCAM-1 の発現誘導によりリンパ球の血管接着促進 ケモカイン (IL-8 や MCP-1) の産生亢進による白血球遊走促進 肝細胞から CRP 産生の誘導 脂肪細胞の分泌するアディポカインの一つ
IL-8	上皮細胞 血管内皮細胞 マクロファージ	好中球 血管内皮細胞	ケモカインとして白血球遊走を促進
IL-10	単球／マクロファージ T/B 細胞	単球／マクロファージ	MHC Class II，補助刺激分子の発現抑制 B 細胞の分化，抗体産生の増強 IFN- γ 産生の抑制により Th2 応答を促進
IL-12	マクロファージ	T 細胞 NK 細胞	Th1 応答を促進
IL-17	T 細胞 (Th17)	T/B 細胞 マクロファージ 好中球	IL-6，COX-2，NO 産生を誘導 自己免疫疾患においても観察される 好中球前駆細胞を分化させる
IL-23	マクロファージ 樹状細胞	T 細胞	Th17 への分化誘導
TNF- α	マクロファージ NK 細胞 脂肪細胞	NK 細胞 マクロファージ	細胞増殖・分化を誘導 アポトーシスを誘導 脂肪細胞の分泌するアディポカインの一つ
IFN- γ	T 細胞 (Th1) NK 細胞 T 細胞 (Tc)	マクロファージ T 細胞 抗原提示細胞 (マクロファージ，B 細胞，樹状細胞)	マクロファージの活性化（リソソームの活性化） NK 細胞の活性化 抗原提示能の増強
TGF- β	T 細胞 マクロファージ	T/B 細胞 単　球	広範な細胞種の増殖・分化を誘導 骨芽細胞増殖

1-5

歯周病原細菌による免疫応答のかく乱

これまで述べてきたように、歯周炎組織では活発な免疫応答が生じている。それにもかかわらず病原菌の排除ができない結果、炎症状態が慢性化しているために結合組織破壊と歯槽骨吸収が終息しないということが考えられる。もっとも大きな原因は歯周病原細菌がバイオフィルムを形成し、貪食にも抗体にもその他の抗菌ペプチドにも抵抗性を示し、自然免疫系、適応免疫系いずれも効果的に作用していないことが挙げられる。それと同時に、ある種の歯周病原細菌のもつ免疫かく乱作用が、歯周組織における免疫系のバランスを乱していることが明らかになってきた。

細菌感染はTLRをはじめとするpattern recognition receptorによって認識される。TLRは単独ではなく、その他のさまざまな受容体分子と複合体をなして最適に機能するよう調整されている。しかし、*P. gingivalis*にはそれらと拮抗するような受容体応答を誘導したり、受容体認識後のシグナル伝達を調整する分子に作用して免疫細胞の応答性を乱したりするものがあることがわかった。

*P. gingivalis*の線毛(FimA fimbriae)はマクロファージのケモカイン受容体CXCR4と結合することにより、TLR2を介した炎症性サイトカイン産生や殺菌作用をもつNO_2^-の産生を抑制することが報告されている。FimA fimbriaeは細胞膜上でCXCR4とTLR2の相互作用を誘導し、cyclic AMPを介したprotein kinase(プロテインキナーゼ)Aの作用によりTLRのシグナリングを抑制する。

また、*P. gingivalis*のTLR2を介したシグナルは補体受容体CR3の活性化(高親和性)を誘導し、CR3と*P. gingivalis*の結合はIL-12の産生抑制を誘導する。さらに、*P. gingivalis*のもつ強力なタンパク分解酵素ジンジパインは補体成分C5をC5aとC5bに分解するが、C5aはC5a受容体を介してCXCR4と同様、cyclic AMPを介したプロテインキナーゼAの活性化によりNO_2^-の産生を抑制する[21]。

LPSはグラム陰性菌の代表的な病原因子で、強い炎症性サイトカイン誘導活性をもつことが知られているが*P. gingivalis*のLPSは大腸菌のLPSと比較してその活性が非常に弱い。*P. gingivalis* LPSはTLRシグナル伝達経路において負の制御機構を担う分子IL-1 receptor-associated kinase M(IRAK-M)を特異的に活性化し、結果としてNF-κBの活性を抑制することで炎症性サイトカインの産生誘導を抑えていることが明らかになっている。このような機能は*P. gingivalis*が免疫監視機構をかいくぐり、局所からの排除を逃れることに貢献し、結果として炎症の慢性化にかかわっていると考えられる[22]。

■参考文献■

1. Devine DA and Cosseau C. Antimicrobial host defence peptides in oral health and periodontitis. In : Henderson B, Curtis MA, Seymour R, Donos N(eds). Periodontal Medicine and Systems Biology. Oxford : Wiley-Blackwell, 2009 ; 279-297.
2. Darveau, RP. Innate immunity and homeostasis in the periodontium. In : Henderson B, Curtis MA, Seymour R, Donos N (eds). Periodontal Medicine and Systems Biology. Oxford : Wiley-Blackwell, 2009 ; 263-277.
3. Mathur A and Michalowicz BS. Cell-Mediated Immune System Regulation in Periodontal Diseases. Crit Rev Oral Biol Med 1997 ; 8 : 76-89.
4. Trinchieri G and Sher A. Cooperation of Toll-like receptor signals in innate immune defence. Nat Rev Immunol 2007 ; 7 : 179-90.
5. Mahanonda R and Pichyangkul S. Toll-like receptors and their role in periodontal health and disease. Periodontol 2000 2007 ; 43 : 41-55.
6. Cutler CW and Jotwani R. Dendritic cells at the oral mucosal interface. J Dent Res 2006 ; 85 : 678-689.
7. Yamazaki K and Nakajima T. Antigen specificity and T-cell clonality in periodontal disease. Periodontol 2000 2004 ; 35 : 75-100.
8. Seymour GJ, Powell RN, Davies WI. Conversion of a stable T-cell lesion to a progressive B-cell lesion in the pathogenesis of chronic inflammatory periodontal disease: an hypothesis. J Clin Periodontol 1979 ; 6 : 267-277.
9. Baker PJ, Garneau J, Howe L, Roopenian DC. T-cell contributions to alveolar bone loss in response to oral infection with *Porphyromonas gingivalis*. Acta Odontol Scand 2001 ; 59 : 222-225.
10. Yamazaki K, Yoshie H, Seymour GJ. T cell regulation of the immune response to infection in periodontal diseases. Histol Histopathol 2003 ; 18 : 889-896.
11. Steinman L. A brief history of T_H17, the first major revision in the T_H1/T_H2 hypothesis of T cell-mediated tissue damage. Nat Med 2007 ; 3 : 139-145.
12. Gaffen SL and Hajishengallis G. A new inflammatory cytokine on the block: re-thinking periodontal disease and the Th1/Th2 paradigm in the context of Th17 cells and IL-17. J Dent Res 2008 ; 87 : 817-828.
13. Petit MD, Hovenkamp E, Hamann D, Roos MT, van der Velden U, Miedema F, Loos BG. Phenotypical and functional analysis of T cells in periodontitis. J Periodont Res 2001 ; 36 : 214-220.
14. Nakajima T, Ueki-Maruyama K, Oda T, Ohsawa Y, Ito H, Seymour GJ, Yamazaki K. Regulatory T-cells infiltrate periodontal disease tissues. J Dent Res 2005 ; 84 : 639-643.
15. Okui T, Ito H, Honda T, Amanuma R, Yoshie H, Yamazaki K. Characterization of $CD4^+$ $FOXP3^+$ T-cell clones established from chronic inflammatory lesions. Oral Microbiol Immunol 2008 ; 3 : 49-54.
16. Ernst CW, Lee JE, Nakanishi T, Karimbux NY, Rezende TM, Stashenko P, Seki M, Taubman MA, Kawai T. Diminished forkhead box P3/CD25 double-positive T regulatory cells are associated with the increased nuclear factor-kappaB ligand ($RANKL^+$) T cells in bone resorption lesion of periodontal disease. Clin Exp Immunol 2007 ; 148 : 271-280.
17. Yamazaki K, Ohsawa Y, Yoshie H. Elevated proportion of natural killer T cells in periodontitis lesions : a common feature of chronic inflammatory diseases. Am J Pathol 2001 ; 158 : 1391-1398.
18. Galli G, Nuti S, Tavarini S, Galli-Stampino L, De Lalla C, Casorati G, Dellabona P, Abrignani S. CD1d-restricted help to B cells by human invariant natural killer T lymphocytes. J Exp Med 2003 ; 197 : 1051-1057.
19. Yamazaki K, Ohsawa Y, Tabeta K, Ito H, Ueki K, Oda T, Yoshie H, Seymour GJ. Accumulation of human heat shock protein 60-reactive T cells in the gingival tissues of periodontitis patients. Infect Immun 2002 ; 70 : 2492-2501.
20. Kornman KS, Page RC, Tonetti MS. The host response to the microbial challenge in periodontitis: assembling the players. Periodontol 2000 1997 ; 14 : 33-53.
21. Hajishengallis G. Complement and periodontitis. Biochem Pharmacol 2010 ; 80 : 1992-2001.
22. Domon H, Honda T, Oda T, Yoshie H, Yamazaki K. Early and preferential induction of IL-1 receptor-associated kinase-M in THP-1 cells by LPS derived from *Porphyromonas gingivalis*. J Leukoc Biol 2008 ; 83 : 672-679.

10 ten | Tooth Regenerative Therapy as an Organ Replacement Regenerative Therapy

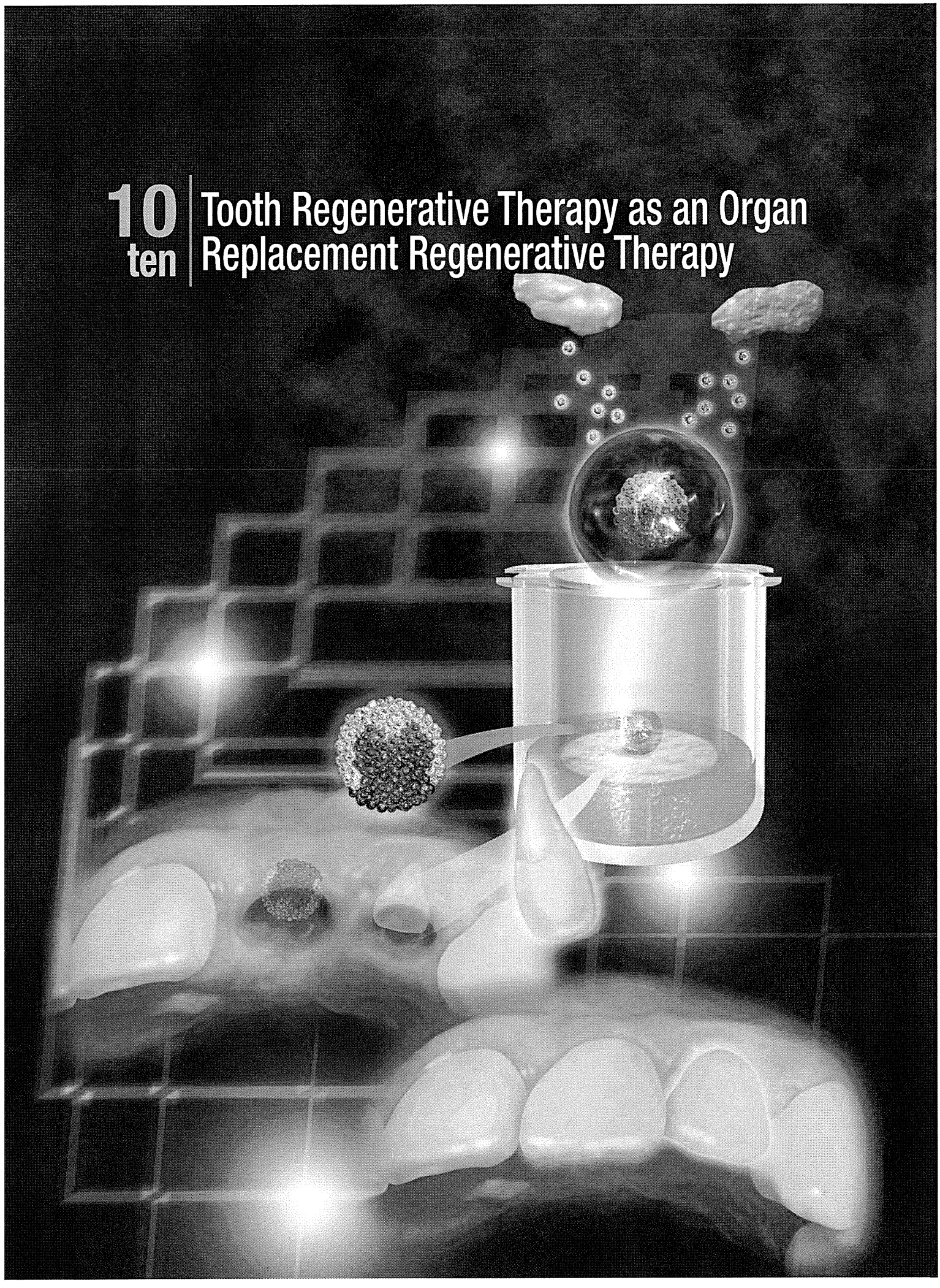

Development of regenerative therapies is expected to create innovative medical therapeutic systems in the 21st century. Tooth development begins with the tooth germ, or *tooth bud*, which is generated by epithelial-menechymal interactions during the embryonic stage of development. It is a highly organized aggregation of cells comprised of several cell types, forming the periodontium, mineralized tooth tissues, and dental pulp. Tooth regeneration has been developed as a model for organ replacement therapy that aims to replace a lost or damaged organ following disease or injury using bioengineered organs.

The current regenerative therapy approach is the transplantation of tissue-derived stem or progenitor cells into the site of the damaged tissue or organ. The ultimate goal of regenerative therapy is the development of a fully functioning bioengineered organ that can replace a lost or damaged organ after injury, disease, or aging.

A tooth is developed from a tooth germ, which is generated by epithelial-menechymal interactions at the embryonic stage of development. It is a highly organized organ comprised of several kinds of cells forming tooth and periodontium, mineralized tissues and blood vessels. The current strategy for tooth regeneration is the production of a bioengineered tooth germ reconstituted from immature epithelial and mesenchymal cells isolated from the developing tooth germ. The realization of tooth regeneration therapy requires the development of a wide variety of technology, including cell processing technology for reconstituting the tooth germ, identification of cell seeds capable of reconstituting the bioengineered tooth germ, and technology for the regulation of tooth size and morphology.

Organ Germ Method: Development of a Novel Three-Dimensional Cell Processing Method for Bioengineered Tooth Germs

A three-dimensional single-cell processing method has been developed for the production of bioengineered tooth germs and is called the *organ germ method.* It is a first step in the evolution of tooth regenerative therapy (Figs 10-1 and 10-2). A bioengineered tooth germ was reconstituted using dissociated dental epithelial and mesenchymal cells with correct cell compartmentalization at high-cell density in collagen gel. The bioengineered tooth germ could regenerate structurally correct tooth at a high frequency when transplanted into the subrenal capsule (Fig 10-3). The structurally correct tooth could also be regenerated from the bioengineered germ in an in vitro organ culture (Fig 10-4).

Fig 10-1 Steps in the development of three-dimensional cell processing technology (the organ germ method) to regenerate a bioengineered tooth germ. Epithelial and mesenchymal tissues were isolated from incisor tooth germ of ED14.5 mice and completely dissociated into epithelial and mesenchymal cells, respectively.

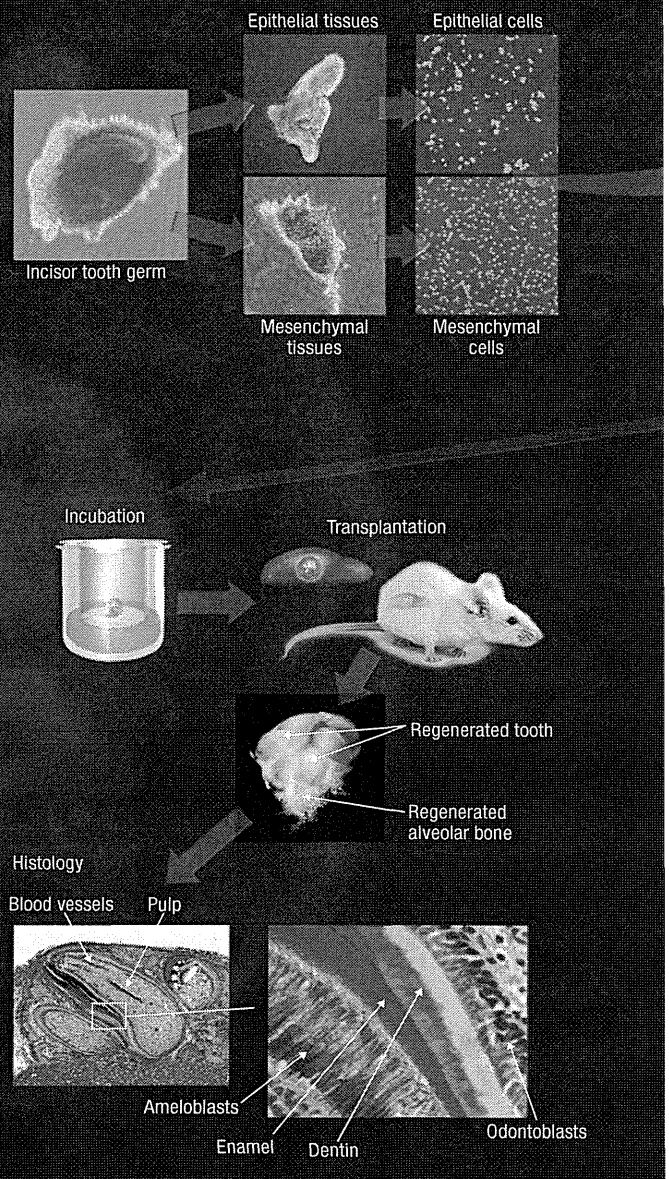

Fig 10-3 Development of bioengineered tooth germ in vivo after subrenal capsule transplantation. Bioengineered tooth germ was incubated for several days with organ culture. Bioengineered tooth germ was transplanted into a subrenal capsule for 14 days. Bioengineered tooth and alveolar bone with correct tooth structure were observed 14 days after transplantation in the subrenal capsule.

Fig 10-2 Epithelial and mesenchymal cells at high cell density were successively injected into collagen gel. The bioengineered tooth germ was reconstituted using epithelial and mesenchymal cells with correct cell compartmentalization at high cell density.

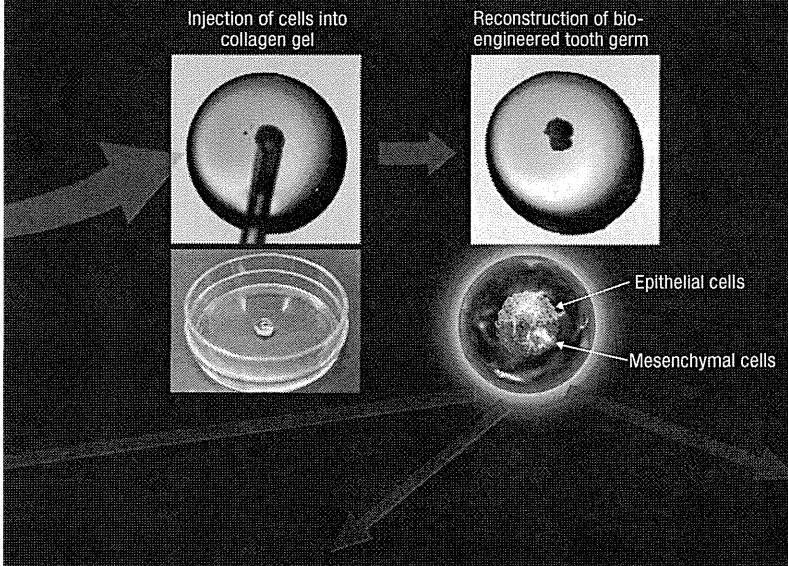

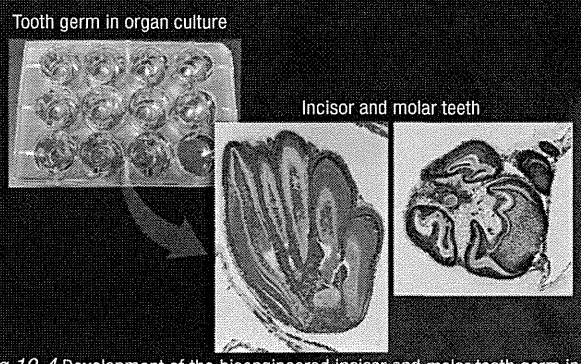

Fig 10-4 Development of the bioengineered incisor and molar tooth germ in vitro in organ culture. Bioengineered tooth germ was cultured in vitro for 14 days in organ culture. Incisor and molar teeth were formed from the respective bioengineered germs.

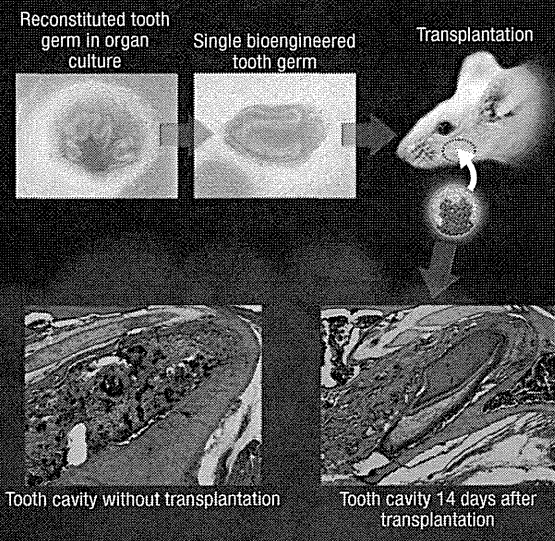

Fig 10-5 A bioengineered tooth was developed after transplantation of the bioengineered tooth germ into the tooth cavity of adult mice. The reconstituted tooth germ was cultured for several days in an in vitro organ culture. Isolation of single bioengineered tooth germ by microsurgery. Transplantation of the bioengineered tooth germ into the tooth cavity of an adult mouse. Histological analysis of the tooth cavity without transplantation. Histological analysis of the tooth cavity 14 days after transplantation of the bioengineered tooth germ.

Analysis of the Development of the Bioengineered Tooth Germ in an Adult Oral Environment

The bioengineered tooth germ could also generate a structurally correct tooth after transplantation under a tooth cavity of adult mice showing penetrations of nerve fibers and blood vessels (Fig 10-5). Our results demonstrate the potential of bioengineered tooth replacement by transplantation of the bioengineered tooth germ in adult oral environment for use in future organ replacement regenerative therapy.

Moreover, a feasibility study of the realization of tooth regeneration therapy has been performed in collaboration with dental research organizations. Further studies on the identification of adult tissue-derived cell seeds for the reconstitution of the bioengineered tooth germ, initiation signals for tooth development, and regeneration of periodontium and tooth root will help to achieve the realization of tooth regenerative therapy for missing teeth. These technical achievements will make substantial contributions to the development of bioengineering technology for future organ-replacement regenerative therapy and to an improved quality of life for many people.

Recommended Reading

1. Nakao K, Morita R, Saji Y, et al. The development of a bioengineered organ germ method. Nat Methods 2007;4:227–230.

2. Komine A, Suenaga M, Nakao K, Tsuji T, Tomooka Y. Tooth regeneration from newly established cell lines from a molar tooth germ epithelium. Biochem Biophys Res Commun 2007;355:758–763.

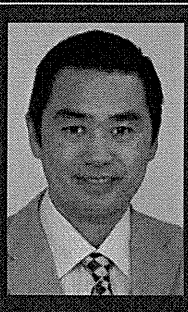

Masahiro Saito, DDS, PhD

Associate Professor
Department of Biological Science and Technology
Research Institute for Science and Technology
Tokyo University of Science
Tokyo, Japan

Takashi Tsuji, PhD

Professor
Department of Biological Science and Technology
Research Institute for Science and Technology
Tokyo University of Science
Tokyo, Japan

Biochemical and Biophysical Research Communications 426 (2012) 643–648

Contents lists available at SciVerse ScienceDirect

Biochemical and Biophysical Research Communications

journal homepage: www.elsevier.com/locate/ybbrc

Role of ferritin in the cytodifferentiation of periodontal ligament cells

Jianxia Hou [a,b], Satoru Yamada [b,*], Tetsuhiro Kajikawa [b], Nobuhiro Ozaki [b], Toshihito Awata [b], Satoko Yamaba [b], Shinya Murakami [b]

[a] Department of Periodontology, Peking University School and Hospital of Stomatology, 22 Zhongguancun Nandajie, Haidian District, Beijing 100081, PR China
[b] Department of Periodontology, Osaka University Graduate School of Dentistry, 1-8 Yamadaoka, Suita, Osaka 565-0871, Japan

ARTICLE INFO

Article history:
Received 29 August 2012
Available online 11 September 2012

Keywords:
Periodontal ligament
Ferritin
Osteogenesis
Cementogenesis

ABSTRACT

This study investigated the expression and functions of ferritin, which is involved in osteoblastogenesis, in the periodontal ligament (PDL). The PDL is one of the most important tissues for maintaining the homeostasis of teeth and tooth-supporting tissues. Real-time PCR analyses of the human PDL revealed abundant expression of *ferritin light polypeptide* (*FTL*) and *ferritin heavy polypeptide* (*FTH*), which encode the highly-conserved iron storage protein, ferritin. Immunohistochemical staining demonstrated predominant expression of FTL and FTH in mouse PDL tissues *in vivo*. In *in vitro*-maintained mouse PDL cells, FTL and FTH expressions were upregulated at both the mRNA and protein levels during the course of cytodifferentiation and mineralization. Interestingly, stimulation of PDL cells with exogenous apoferritin (iron-free ferritin) increased calcified nodule formation and alkaline phosphatase activity as well as the mRNA expressions of mineralization-related genes during the course of cytodifferentiation. On the other hand, RNA interference of *FTH* inhibited the mineralized nodule formation of PDL cells. This is the first report to demonstrate that ferritin is predominantly expressed in PDL tissues and positively regulates the cytodifferentiation and mineralization of PDL cells.

1. Introduction

The periodontal ligament (PDL) is a specialized connective tissue interposed between the roots of teeth and the inner wall of tooth-supporting bone (alveolar bone). The PDL links the teeth to the alveolar bone proper, thereby providing support, protection and sensory input for the masticatory system [1]. It has also been demonstrated that PDL tissues contain multipotent mesenchymal stem cells that can differentiate into mineralized tissue-forming cells, such as osteoblasts and cementoblasts [2,3]. Thus, the PDL is thought to play crucial roles for not only homeostasis of periodontal tissues but also bone remodeling, wound healing and tissue regeneration [1]. Recent reports have demonstrated that ferritin, a key molecule for controlling the iron concentration, regulates osteoblast differentiation [4,5]. Cytosolic ferritin is a ubiquitous and highly conserved iron storage molecule that is composed of ferritin light polypeptide (FTL) and ferritin heavy polypeptide (FTH) [6]. Twenty-four ferritin subunits assemble to form the apoferritin (iron-free ferritin) shell. The FTL and FTH subunits are encoded by separate genes and their functions are nonexchangeable [7,8].

In the present study, we investigated the expression of ferritin in the PDL to clarify the molecular characteristics of PDL cells. Interestingly, we found that FTL and FTH were highly expressed in PDL tissues *in vivo* and elucidated the function of ferritin for the cytodifferentiation of PDL cells *in vitro*.

2. Materials and methods

2.1. RNA extraction and real-time PCR analysis

The clinical study was performed with appropriate approval from the Institutional Ethics Committee, and informed consent was obtained from all patients. Total RNA was extracted from cultured cells and human PDL tissues freshly isolated from an extracted first premolar of patients undergoing tooth extraction using RNA Bee (Tel-Test, Friendswood, TX) according to the manufacturer's protocol. Human tissue total RNAs (heart, skin, kidney, bone marrow, spleen, testis, lung, liver, skeletal muscle, brain and thymus) were purchased from Bio Chain (Hayward, CA). cDNA was synthesized from the purified total RNA using a High Capacity cDNA Reverse Transcription Kit (Applied Biosystems, Carlsbad, CA) according to the manufacturer's instructions. The obtained cDNA was mixed with Power PCR SYBR Master Mix (Applied Biosystems) and gene-specific primers (Takara Bio, Shiga, Japan). The nucleotide

Abbreviations: PDL, periodontal ligament; FTL, ferritin light polypeptide; FTH, ferritin heavy polypeptide; ALPase, alkaline phosphatase.

* Corresponding author. Fax: +81 6 6879 2934.
E-mail addresses: jxhou@163.com (J. Hou), satoru@dent.osaka-u.ac.jp (S. Yamada), t-kajik@dent.osaka-u.ac.jp (T. Kajikawa), n-ozaki@dent.osaka-u.ac.jp (N. Ozaki), tawata@dent.osaka-u.ac.jp (T. Awata), skawa@dent.osaka-u.ac.jp (S. Yamaba), ipshinya@dent.osaka-u.ac.jp (S. Murakami).

0006-291X/$ - see front matter © 2012 Elsevier Inc. All rights reserved.
http://dx.doi.org/10.1016/j.bbrc.2012.09.008

sequences of the primers are shown in Table 1. Real-time PCR was performed using a 7300 Fast Real-time RT-PCR System (Applied Biosystems) according to the manufacturer's instructions. The amplification conditions consisted of an initial 15 min denaturation step at 95 °C, followed by 40 cycles of denaturation at 94 °C for 15 s, annealing at 60 °C for 30 s and elongation at 72 °C for 30 s. The dissociation curves were analyzed to ensure the amplification of a single PCR product in each case. The relative expression levels were calculated by normalization for the gene expression of *hypoxanthine phosphoribosyl transferase* (*HPRT*) for human genes and *glyceraldehyde-3-phosphate dehydrogenase* (*GAPDH*) for mouse genes.

2.2. Tissue preparation and immunohistochemical staining

The animal experiments were approved by the Institutional Animal Care and Use Committee. Eight-week-old C57BL/6 mice were anesthetized by intraperitoneal injection of Nembutal (50 mg/kg body weight). Next, intracardial perfusion was performed with physiological saline containing 5 U/ml heparin (Aventis Pharma, Tokyo, Japan) for 2–3 min, followed by perfusion with 5% paraformaldehyde in 0.1 M sodium phosphate buffer (pH 7.4) at 4 °C for 15 min. Upper jaw samples containing teeth were excised, and most of the soft tissue was removed. All of the samples were further fixed by immersion in the above fixative overnight at 4 °C and then demineralized in buffered 10% EDTA at 4 °C under agitation for 7 days. The EDTA solution was changed daily. The samples were then embedded in OCT compound (Sakura Finetek USA, Torrance, CA) on dry ice. Serial 14 μm sections of the second molars were cut and mounted on aminopropylsilane-coated slides. Endogenous peroxidase activity was inactivated by incubation with 0.3% H_2O_2 in PBS containing 0.3% FBS (Nichirei Bioscience, Tokyo, Japan) for 30 min at room temperature. After blocking with 3% BSA (Kirkegaard & Perry Laboratories, Gaithersburg, MD) in PBS overnight at 4 °C, immunohistochemical staining was carried out following standard procedures. A goat anti-FTL polyclonal antibody (1:1000) and a rabbit anti-FTH polyclonal antibody (1:1000) were purchased from Santa Cruz Biotechnology (Santa Cruz, CA) and used as the primary antibodies. Normal goat IgG and rabbit IgG (Vector Laboratories, Burlingame, CA) served as controls for the primary antibodies. The incubations were carried out overnight at 4 °C. After washing, the sections were reacted with biotinylated anti-goat IgG and biotinylated anti-rabbit IgG secondary antibodies (Vector Laboratories) for 90 min at room temperature. A Vectastain Avidin–Biotin Complex Kit (Vector Laboratories) and DAB solution (20 mg DAB, 50 ml PBS, 4.5 μl H_2O_2) were used for signal detection. Counterstaining was performed with Mayer's Hematoxylin (Muto Pure Chemicals Ltd., Tokyo, Japan).

2.3. Cell culture and induction of PDL cell cytodifferentiation and mineralization

We established a mouse PDL cell line, MPDL22, and a mouse gingival fibroblast cell line, MG/B6. We maintained these cells as previously described [9]. A preosteoblastic cell line, KUSA-A1, was obtained from Riken Cell Bank (Tsukuba, Japan) [10]. For differentiation of these cells into hard tissue-forming cells *in vitro*, we cultured the cells in 12-well plates until they reached confluence. At this point, we replaced the standard medium with α-MEM supplemented with 10% FCS, 10 mM β-glycerophosphate and 50 μg/ml ascorbic acid (mineralization-inducing medium). Apoferritin (Sigma–Aldrich, St. Louis, MO) was added to the mineralization-inducing medium at various concentrations.

2.4. Western blotting analysis of FTL and FTH in PDL cells

MPDL22 cells cultured in the mineralization-inducing medium were lysed with RIPA lysis buffer (Millipore, Billerica, MA). The protein concentrations of the cell lysates were measured using a Bradford 595 assay (Bio-Rad, Hercules, CA) according to the manufacturer's instructions. Aliquots of the cell lysates (30 μg protein) were separated by 12% SDS–PAGE and transferred onto polyvinylidene difluoride membranes. The membranes were blocked in TBST (50 mM Tris–HCl pH 7.5, 150 mM NaCl, 0.1% (v/v) Tween-20) containing 5% (w/v) nonfat dried milk at 4 °C overnight. The above-described goat anti-FTL and rabbit anti-FTH polyclonal antibodies were used as the primary antibodies at a dilution of 1:1000. Briefly, after three washes in TBST, the membranes were incubated with the primary antibodies in TBST containing 5% milk overnight at 4 °C. After three further washes in TBST, the membranes were incubated with horseradish peroxidase-linked donkey anti-goat IgG and goat anti-rabbit IgG secondary antibodies (Research & Diagnostics Systems Inc., Minneapolis, MN) for 60 min at room temperature. The immunoreactive proteins were detected using an ECL Plus Kit (GE Healthcare, Piscataway, NJ) according to the manufacturer's instructions.

2.5. Alizarin red staining, and determination of the alkaline phosphatase (ALPase) activity and cellular DNA content

Histochemical staining of Ca^{2+} was performed by a modification of the method described by Dahl et al. [11]. ALPase activity was assessed according to the procedure of Bessay et al. and DNA content was measured using a modification of the method of Labarca and Pagien as previously described [12].

2.6. RNA interference

Short hairpin RNA (shRNA) plasmids for the mouse *FTH* gene (shFTH) and a negative control (shControl) were purchased from Santa Cruz Biotechnology. For stable transfection, we plated 2×10^6 MPDL22 cells/well in 6-well plates. After 12 h, the cells were transfected with the shFTH and shControl plasmids, respectively, using Nucleofector kit R reagent (Lonza, Basel, Switzerland) in accordance with the manufacturer's protocol. After 24 h, puromycin (2 μg/ml) was added to the culture medium to initiate drug selection. After the selection, *FTH* expression was evaluated by

Table 1
Nucleotide sequences of the primers used for real-time PCR analysis.

Gene	Forward primer	Reverse primer
Human *FTL*	5′-ACCATGAGCTCCCAGATTCGTC-3′	5′-CACATCATCGCGGTCGAAATAG-3′
Human *FTH*	5′-CAGGTGCGCCAGAACTACCA-3′	5′-CCACATCATCGCGGTCAAAG-3′
Human *HPRT*	5′-GGCAGTATAATCCAAAGATGGTCAA-3′	5′-GTCAAGGGCATATCCTACAACAAAC-3′
Mouse *FTL*	5′-CCGTGCACTCTTCCAGGATGT-3′	5′-CCTTATCCAGATAGTGGCTTTCCAG-3′
Mouse *FTH*	5′-TGCGCCAGAACTACCACCAG-3′	5′-AGAGCCACATCATCTCGGTCAA-3′
Mouse *Runx2*	5′-CACTGGCGGTGCAACAAGA-3′	5′-TTTCATAACAGCGGAGGCATTTC-3′
Mouse *type 1 collagen*	5′-CAGGGTATTGCTGGACAACGTG-3′	5′-GGACCTTGTTTGCCAGGTTCA-3′
Mouse *osteocalcin*	5′-AGCAGCTTGGCCCAGACCTA-3′	5′-TAGCGCCGGAGTCTGTTCACTAC-3′
Mouse *GAPDH*	5′-TGTGTCCGTCGTGGATCTGA-3′	5′-TTGCTGTTGAAGTCGCAGGAG-3′

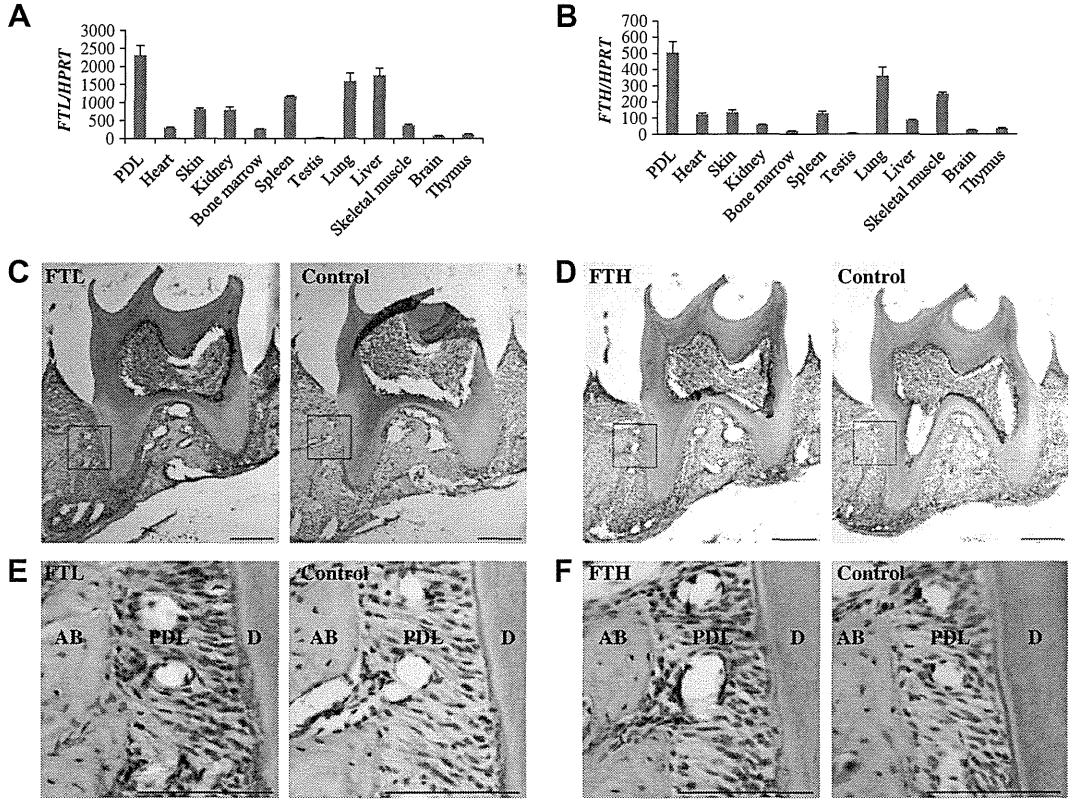

Fig. 1. Expression of FTL and FTH in human and mouse PDL tissues. (A, B) Real-time PCR was performed for the gene expression of *FTL* (A) and *FTH* (B) in various human tissues. The expressions of *FTH* and *FTL* were normalized by the expression of *HPRT*. The data represent the means ± SD of triplicate assays. (C, D) Immunohistochemical analyses of FTL (C) and FTH (D) in the maxilla of 8-week-old C57BL/6 mice. Scale bars, 200 μm. (E, F) Panels (E) and (F) show higher magnification images of the boxed areas in panels (C) and (D), respectively. Scale bars, 100 μm. AB, alveolar bone; PDL, periodontal ligament; D, dentin.

real-time PCR. Stable transfectants with *FTH* knockdown were then established.

2.7. Phosphate measurement

Cells were washed twice with PBS and solubilized with RIPA lysis buffer (Millipore). The Pi contents of the cell lysates were measured using a QuantiChrome Phosphate Assay Kit (BioAssay Systems, Hayward, CA). The phosphate contents of the cells were normalized by the protein contents and expressed as μM/mg cell protein.

2.8. Statistical analysis

The results were presented as means ± SD. Statistical analyses were carried out using Student's *t*-test for paired comparisons with the software Excel Statistics (SSRI, Tokyo, Japan). Values of $P < 0.05$ were considered statistically significant.

3. Results

3.1. FTL and FTH are highly expressed in human and mouse PDL tissues

First, we analyzed *FTL* and *FTH* expression in various human tissues. Real-time PCR analyses revealed markedly higher expression levels of *FTL* and *FTH* in the PDL than in the other human tissues examined (Fig. 1A and B). These findings prompted us to investigate the specific expression of FTL and FTH in periodontal tissues *in vivo*. We carried out immunohistochemical analyses of FTL and FTH expression in mouse maxilla specimens. FTL and FTH were both predominantly expressed in the PDL tissues (Fig. 1C–F). Expression of FTL and FTL was also observed in other soft tissues, such as the dental pulp and gingiva, but at much lower levels than in the PDL tissues.

3.2. FTL and FTH expressions are induced during PDL cell cytodifferentiation in vitro

To clarify a more complete expression pattern of FTL and FTH, we analyzed the FTL and FTH mRNA and protein expression levels during cytodifferentiation of the mouse PDL cell line MPDL22. Expression of *FTL* and *FTH* mRNAs and FTL and FTH proteins was induced during the course of MPDL22 cytodifferentiation and peaked at the early stage of the cytodifferentiation (Fig. 2). *GAPDH* mRNA expression was stable during the course of the MPDL22 cytodifferentiation.

3.3. Apoferritin enhances MPDL22 cytodifferentiation and mineralization

To examine the effects of ferritin on the cytodifferentiation and mineralization of PDL cells, we cultured MPDL22 cells in the mineralization-inducing medium in the presence of apoferritin, a kind of iron-free ferritin. First, we checked the effects of apoferritin on the mineralization of the preosteoblastic cell line KUSA-A1. In accordance with previous reports showing inhibitory effects of apoferritin on osteogenesis [4,5], we confirmed that apoferritin inhibited the mineralized nodule formation of KUSA-A1 cells in a dose-dependent manner (Fig. 3A). We also confirmed that apoferritin had no effects on the mouse gingival fibroblast cell line MG/

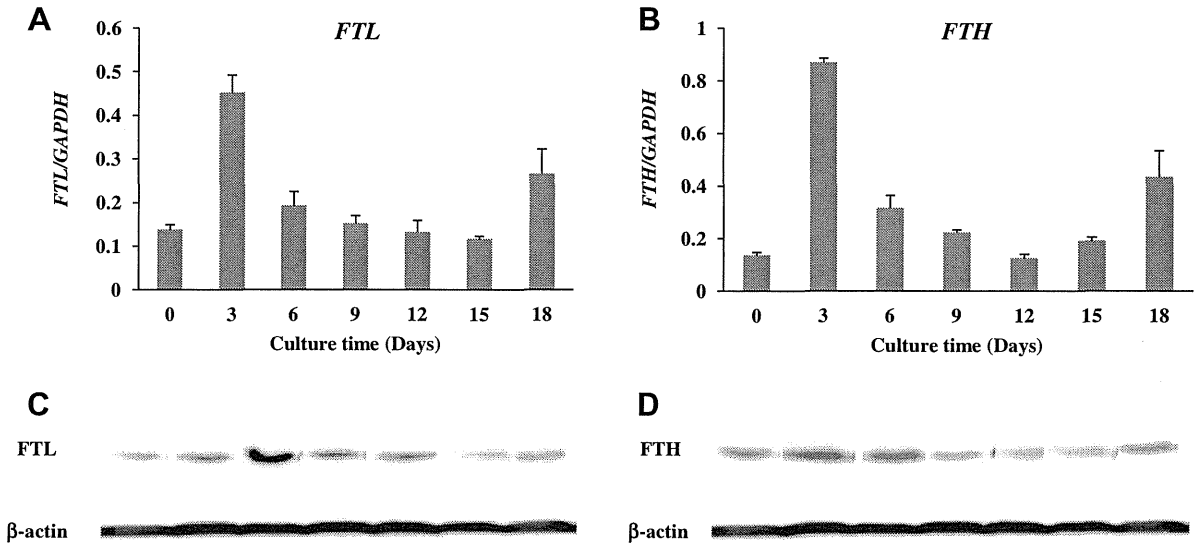

Fig. 2. Induction of FTL and FTH expression during cytodifferentiation of PDL cells. MPDL22 cells were cultured in the mineralization-inducing medium for 18 days. (A, B) Real-time PCR analyses for the gene expression of *FTL* (A) and *FTH* (B). The expression levels of *FTL* and *FTH* were normalized by the expression of *GAPDH*. The data represent the means ± SD of triplicate assays. (C, D) Western blotting analyses for FTL (C) and FTH (D) expression during the cytodifferentiation of MPDL22 cells.

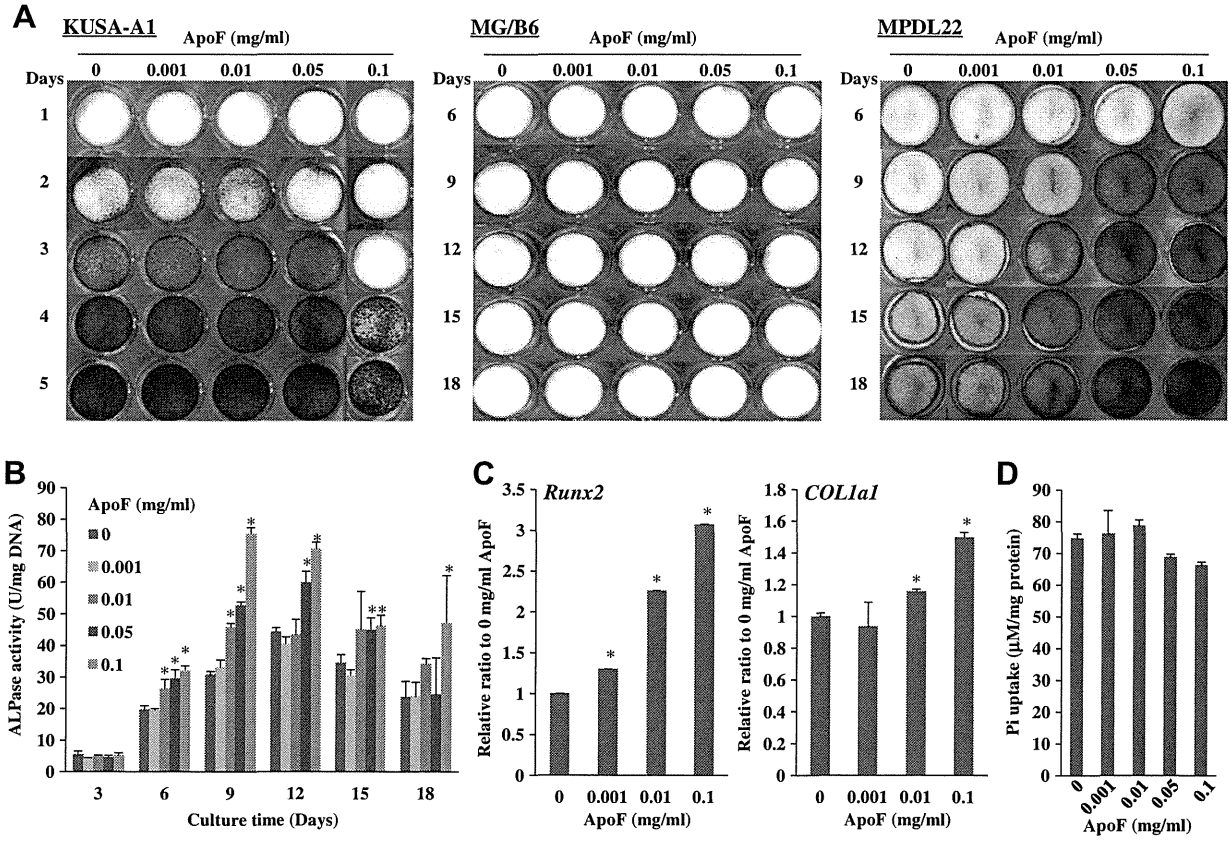

Fig. 3. Apoferritin enhances the cytodifferentiation and mineralization of MPDL22 cells. Cells were cultured in the mineralization-inducing medium alone or supplemented with apoferritin at 0.001, 0.01, 0.05 and 0.1 mg/ml for the indicated days. (A) Apoferritin enhances the mineralized nodule formation of MPDL22 cells in a dose- and time-dependent manner, as indicated by alizarin red staining. On the other hand, apoferritin inhibits the mineralized nodule formation of KUSA-A1 cells. Apoferritin has no effects on the mouse gingival fibroblast cell line MG/B6. (B) Apoferritin increases the ALPase activity of MPDL22 cells in a dose-dependent manner. (C) Real-time PCR was performed for the expression of cytodifferentiation- and mineralization-related genes, namely *Runx2* and *type I collagen*, after stimulation with exogenous apoferritin on day 15. The expression of the indicated genes was normalized by the expression of *GAPDH*. The data represent the means ± SD of triplicate assays. $^{*}P < 0.05$, *vs.* 0 mg/ml apoferritin. (D) Intracellular Pi concentrations are not affected by apoferritin. MPDL22 cells were cultured in the mineralization-inducing medium alone or supplemented with apoferritin at the indicated concentrations for 48 h. Cell lysates were used to measure the Pi levels. The data represent the means ± SD of triplicate assays. ApoF, apoferritin; *COL1a1*, *type I collagen*.

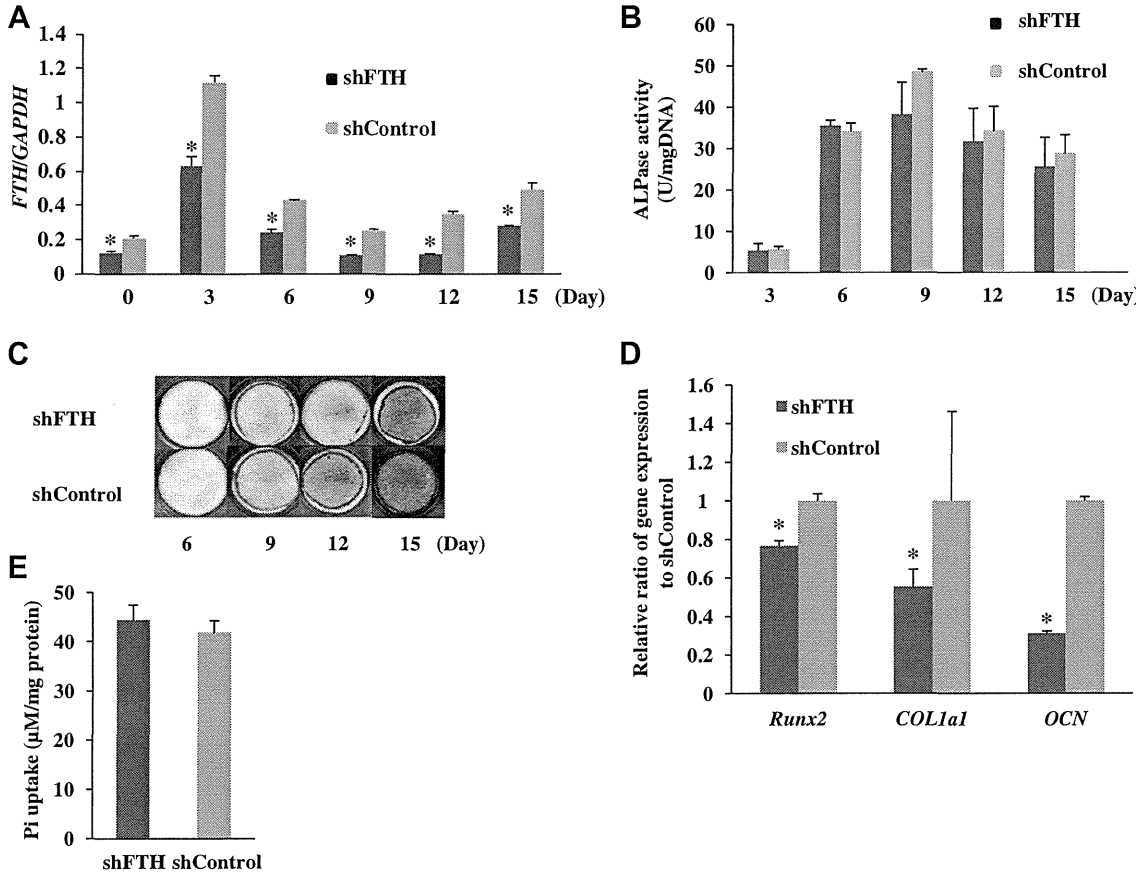

Fig. 4. Stable knockdown of *FTH* suppresses the cytodifferentiation of MPDL22 cells. Transfected MPDL22 cells were cultured in the mineralization-inducing medium for 15 days. (A) Confirmation of stable knockdown of *FTH* by real-time PCR analysis. (B) ALPase activities during the cytodifferentiation course. The data represent the means ± SD of triplicate assays. $^*P < 0.05$, *vs.* shControl transfectants. (C) Suppression of mineralized nodule formation in the *FTH* shRNA transfectants indicated by alizarin red staining. (D) Real-time PCR reveals strong inhibition of cytodifferentiation- and mineralization-inducing gene expression in the *FTH* shRNA transfectants on day 12. The data represent the means ± SD of triplicate assays. $^*P < 0.05$, *vs.* shControl transfectants. (E) No difference in the intracellular Pi concentrations between the *FTH* shRNA and shControl transfectants. The transfectant cells were cultured in the mineralization-inducing medium and cell lysates were used to measure the Pi levels on day 6. The data represent the means ± SD of triplicate assays. *COL1a1*, *type I collagen*; *OCN*, *osteocalcin*.

B6, which has no ability to undergo cytodifferentiation and mineralization (Fig. 3A). On the other hand, apoferritin clearly increased the mineralized nodule formation during the course of MPDL22 cytodifferentiation in a time- and dose-dependent manner (Fig. 3A). Moreover, apoferritin significantly increased the ALPase activity in a dose-dependent manner (Fig. 3B). In addition, real-time PCR analyses demonstrated that apoferritin significantly upregulated the gene expressions of *Runx2* and *type I collagen* during MPDL22 cytodifferentiation (Fig. 3C). We confirmed that the intracellular Pi concentrations of MPDL cells were not affected by apoferritin during culture for 48 h (Fig. 3D).

3.4. RNA interference of FTH downregulates MDPL22 cytodifferentiation and mineralization

It has been reported that FTH, which has ferroxidase activity, regulates osteoblast differentiation [4]. Thus, we established MPDL22 cells transfected with a shRNA for the *FTH* gene to examine the effects of *FTH* knockdown on the cytodifferentiation and mineralization of PDL cells. First, we confirmed that the transfectants showed reduced *FTH* expression (Fig. 4A). We then cultured the transfectants in the mineralization-inducing medium and analyzed the ALPase activity and mineralized nodule formation. The *FTH* shRNA transfectants did not show significant decreases in the ALPase activity (Fig. 4B). However, the mineralized nodule formation of the *FTH* shRNA transfectants was significantly inhibited compared with the shControl transfectants (Fig. 4C). In addition, the *FTH* shRNA transfectants showed strong downregulation of *Runx2*, *type I collagen* and *osteocalcin* expression, compared with the shControl transfectants (Fig. 4D). There was no difference in the intracellular Pi concentrations between the *FTH* shRNA and shControl transfectants (Fig. 4E).

4. Discussion

Our present data demonstrate for the first time that ferritin is predominantly expressed in the PDL and enhances the cytodifferentiation and mineralization of PDL cells. Considering the fact that the PDL plays crucial roles in the homeostasis, remodeling and regeneration of periodontal tissues, including the alveolar bone and cementum, we speculate that ferritin may be one of the key molecules involved in regulating the specific functions of the PDL.

Iron is essential for many important cellular functions and processes, including the cell cycle, reductive conversion of ribonucleotides to deoxyribonucleotides and electron transport. Ferritin plays a key role in maintaining iron homeostasis by binding and regulating excess intracellular iron. Cytosolic ferritin is a highly conserved

three-dimensional iron storage molecule that can capture up to 4500 Fe^{3+} ions. Each hollow apoferritin (iron-free ferritin) shell is made up of 24 FTL and FTH polypeptide chains [13,14]. Ferritin possesses two well-studied properties as follows: iron incorporation to maintain the balance of cellular iron and ferroxidase activity, an inherent feature of FTH, to promote iron incorporation and oxidize Fe^{2+} into the safer Fe^{3+} form. FTL is associated with iron nucleation, mineralization and long-term iron storage [14,15]. The expression of ferritin is under delicate control at both the transcriptional and posttranscriptional levels [16,17]. Both FTL and FTH are critical for maintaining iron homeostasis. It is well known that tight regulation of iron homeostasis is crucial for not only maintaining normal cellular functions but also preventing iron-mediated oxidative stress [18]. Reactive oxygen species induced by oxidative stress tightly regulate ferritin expression [19]. Hypoxia is also involved in the translational regulation of ferritin [18]. The PDL constitutively receives mechanical stress, such as occlusal pressure, that reduces the blood flow and leads to local hypoxia and reoxygenation [20]. This *in vivo* situation may regulate the expression and function of FTL and FTH, especially in the PDL.

It is well known that iron overload leads to both osteoporosis and osteopenia *via* direct effects on osteoblast activity. Recently, ferritin, especially FTH with ferroxidase activity, has been reported to negatively modulate Pi-mediated calcification and osteoblastic differentiation of human smooth muscle cells and osteosarcoma cells mainly *via* the ferroxidase activity of ferritin [4,5]. The opposing effects of ferritin on PDL cells and other cell lines may arise through different mineralization-inducing environments as well as different cell properties in nature. PDL cells have been reported to differentiate into either osteoblasts or cementoblasts depending on the need and the environment. *In vitro*-maintained PDL cells from rats were found to form mineralized nodules that differed from those formed by osteoblasts [21].

To clarify the role of FTH in PDL cells during the course of their cytodifferentiation and mineralization, we established MPDL22 transfectants with *FTH* knockdown. Downregulation of the cytodifferentiation and mineralization-related genes *Runx2*, *type I collagen* and *osteocalcin* were observed in the *FTH* shRNA transfectants. The *FTH* shRNA also inhibited mineralized nodule formation. We further found that ceruloplasmin, which possesses ferroxidase activity, enhanced the mineralized nodule formation of PDL cells (data not shown). These findings clearly suggest that ferritin, probably through the ferroxidase activity of FTH, regulates the cytodifferentiation and mineralization of PDL cells.

In conclusion, we have demonstrated for the first time that FTL and FTH are predominantly expressed in PDL tissues. Ferritin enhanced the cytodifferentiation and mineralization of PDL cells, at least in part *via* FTH, which possesses ferroxidase activity. These findings suggest that ferritin is involved in the homeostasis, remodeling and regeneration of periodontal tissues. Further characterization of the roles of ferritin in the cytodifferentiation of cells may uncover novel functions for this highly conserved protein.

Acknowledgments

This work was jointly supported by Grants-in-Aid from the Japan Society for the Promotion of Science (Nos. 23249086 and 23390478) and the China Scholarship Council (CSC).

References

[1] W. Beertsen, C.A. McCulloch, J. Sodek, The periodontal ligament: a unique, multifunctional connective tissue, Periodontol 2000 (13) (1997) 20–40.
[2] P.M. Bartold, S. Shi, S. Gronthos, Stem cells and periodontal regeneration, Periodontol 2000 (40) (2006) 164–172.
[3] B.M. Seo, M. Miura, S. Gronthos, P.M. Bartold, S. Batouli, J. Brahim, M. Young, P.G. Robey, C.Y. Wang, S. Shi, Investigation of multipotent postnatal stem cells from human periodontal ligament, Lancet 364 (2004) 149–155.
[4] A. Zarjou, V. Jeney, P. Arosio, M. Poli, E. Zavaczki, G. Balla, J. Balla, Ferritin ferroxidase activity: a potent inhibitor of osteogenesis, J. Bone Miner. Res. 25 (2010) 164–172.
[5] A. Zarjou, V. Jeney, P. Arosio, M. Poli, P. Antal-Szalmas, A. Agarwal, G. Balla, J. Balla, Ferritin prevents calcification and osteoblastic differentiation of vascular smooth muscle cells, J. Am. Soc. Nephrol. 20 (2009) 1254–1263.
[6] F.M. Torti, S.V. Torti, Regulation of ferritin genes and protein, Blood 99 (2002) 3505–3516.
[7] J.H. Caskey, C. Jones, Y.E. Miller, P.A. Seligman, Human ferritin gene is assigned to chromosome 19, Proc. Natl. Acad. Sci. USA 80 (1983) 482–486.
[8] M. Worwood, J.D. Brook, S.J. Cragg, B. Hellkuhl, B.M. Jones, P. Perera, S.H. Roberts, D.J. Shaw, Assignment of human ferritin genes to chromosomes 11 and 19q13.3----19qter, Hum. Genet. 69 (1985) 371–374.
[9] S. Yamada, M. Tomoeda, Y. Ozawa, S. Yoneda, Y. Terashima, K. Ikezawa, S. Ikegawa, M. Saito, S. Toyosawa, S. Murakami, PLAP-1/asporin, a novel negative regulator of periodontal ligament mineralization, J. Biol. Chem. 282 (2007) 23070–23080.
[10] S. Matsumoto, I. Shibuya, S. Kusakari, K. Segawa, T. Uyama, A. Shimada, A. Umezawa, Membranous osteogenesis system modeled with KUSA-A1 mature osteoblasts, Biochim. Biophys. Acta 1725 (2005) 57–63.
[11] L.K. Dahl, A simple and sensitive histochemical method for calcium, Proc. Soc. Exp. Biol. Med. 80 (1952) 474–479.
[12] S. Yamada, S. Murakami, R. Matoba, Y. Ozawa, T. Yokokoji, Y. Nakahira, K. Ikezawa, S. Takayama, K. Matsubara, H. Okada, Expression profile of active genes in human periodontal ligament and isolation of PLAP-1, a novel SLRP family gene, Gene 275 (2001) 279–286.
[13] P.M. Harrison, P. Arosio, The ferritins: molecular properties, iron storage function and cellular regulation, Biochim. Biophys. Acta 1275 (1996) 161–203.
[14] E.C. Theil, Ferritin: structure, gene regulation, and cellular function in animals, plants, and microorganisms, Annu. Rev. Biochem. 56 (1987) 289–315.
[15] P. Rucker, F.M. Torti, S.V. Torti, Role of H and L subunits in mouse ferritin, J. Biol. Chem. 271 (1996) 33352–33357.
[16] M.W. Hentze, T.A. Rouault, S.W. Caughman, A. Dancis, J.B. Harford, R.D. Klausner, A cis-acting element is necessary and sufficient for translational regulation of human ferritin expression in response to iron, Proc. Natl. Acad. Sci. USA 84 (1987) 6730–6734.
[17] J.L. Casey, M.W. Hentze, D.M. Koeller, S.W. Caughman, T.A. Rouault, R.D. Klausner, J.B. Harford, Iron-responsive elements: regulatory RNA sequences that control mRNA levels and translation, Science 240 (1988) 924–928.
[18] P.D. Ray, B.W. Huang, Y. Tsuji, Reactive oxygen species (ROS) homeostasis and redox regulation in cellular signaling, Cell Signal 24 (2012) 981–990.
[19] K. Orino, L. Lehman, Y. Tsuji, H. Ayaki, S.V. Torti, F.M. Torti, Ferritin and the response to oxidative stress, Biochem. J. 357 (2001) 241–247.
[20] Y. Kitase, M. Yokozeki, S. Fujihara, T. Izawa, S. Kuroda, K. Tanimoto, K. Moriyama, E. Tanaka, Analysis of gene expression profiles in human periodontal ligament cells under hypoxia: the protective effect of CC chemokine ligand 2 to oxygen shortage, Arch. Oral. Biol. 54 (2009) 618–624.
[21] M.I. Cho, N. Matsuda, W.L. Lin, A. Moshier, P.R. Ramakrishnan, In vitro formation of mineralized nodules by periodontal ligament cells from the rat, Calcif. Tissue Int. 50 (1992) 459–467.

RESEARCH REPORTS
Clinical

C. Kudo[1], K. Naruishi[1,2], H. Maeda[3], Y. Abiko[4], T. Hino[5], M. Iwata[6], C. Mitsuhashi[6], S. Murakami[7], T. Nagasawa[8,9], T. Nagata[10], S. Yoneda[10], Y. Nomura[11], T. Noguchi[12], Y. Numabe[13], Y. Ogata[14], T. Sato[15], H. Shimauchi[16], K. Yamazaki[17], A. Yoshimura[18], and S. Takashiba[3]*

[1]Department of Periodontics and Endodontics, Okayama University Hospital, Okayama, Japan; [2]currently, Division of Endodontology, Iwate Medical University, Department of Conservative Dentistry and Oral Rehabilitation, Iwate, Japan; [3]Department of Pathophysiology - Periodontal Science, Okayama, University Graduate School of Medicine, Dentistry and Pharmaceutical Sciences, Okayama, Japan; [4]Department of Biochemistry and Molecular Biology, Nihon University School of Dentistry at Matsudo, Chiba, Japan; [5]Department of Periodontal Medicine, Hiroshima University Graduate School of Biomedical Sciences, Hiroshima, Japan; [6]Toyota Motor Corporation, Tokyo/Aichi, Japan; [7]Department of Periodontology, Division of Oral Biology and Disease Control, Osaka University Graduate School of Dentistry, Osaka, Japan; [8]Department of Hard Tissue Engineering, Tokyo Medical and Dental University Graduate School, Tokyo, Japan; [9]currently, Department of Oral Rehabilitation, Division of Periodontology and Endodontology, School of Dentistry, Health Sciences University of Hokkaido, Hokkaido, Japan; [10]Department of Periodontology and Endodontology, Institute of Health Biosciences, The University of Tokushima Graduate School, Tokushima, Japan; [11]Department of Translational Research, School of Dental Medicine, Tsurumi University, Kanagawa, Japan; [12]Department of Periodontology, School of Dentistry, Aichi-Gakuin University, Aichi, Japan; [13]Department of Periodontology, School of Life Dentistry at Tokyo, Nippon Dental University, Tokyo, Japan; [14]Department of Periodontology, Nihon University School of Dentistry at Matsudo, Chiba, Japan; [15]Department of Oral Health, School of Life Dentistry at Tokyo, Nippon Dental University, Tokyo, Japan; [16]Department of Oral Biology, Division of Periodontology and Endodontology, Tohoku University Graduate School of Dentistry, Miyagi, Japan; [17]Laboratory of Periodontology and Immunology, Department of Oral Health and Welfare, Niigata University Faculty of Dentistry, Niigata, Japan; and [18]Department of Periodontology, Nagasaki University Graduate School of Biomedical Sciences, Nagasaki, Japan; *corresponding author, stakashi@okayama-u.ac.jp

J Dent Res 91(12):1190-1195, 2012

ABSTRACT

Chronic periodontitis is a silent infectious disease prevalent worldwide and affects lifestyle-related diseases. Therefore, efficient screening of patients is essential for general health. This study was performed to evaluate prospectively the diagnostic utility of a blood IgG antibody titer test against periodontal pathogens. Oral examination was performed, and IgG titers against periodontal pathogens were measured by ELISA in 1,387 individuals. The cut-off value of the IgG titer was determined in receiver operating characteristic curve analysis, and changes in periodontal clinical parameters and IgG titers by periodontal treatment were evaluated. The relationships between IgG titers and severity of periodontitis were analyzed. The best cut-off value of IgG titer against *Porphyromonas gingivalis* for screening periodontitis was 1.682. Both clinical parameters and IgG titers decreased significantly under periodontal treatment. IgG titers of periodontitis patients were significantly higher than those of healthy controls, especially in those with sites of probing pocket depth over 4 mm. Multiplied cut-off values were useful to select patients with severe periodontitis. A blood IgG antibody titer test for *Porphyromonas gingivalis* is useful to screen hitherto chronic periodontitis patients (ClinicalTrials.gov number NCT01658475).

KEY WORDS: periodontopathic bacteria, *Porphyromonas gingivalis*, fingertip blood, screening test, cut-off value, multicenter trials.

DOI: 10.1177/0022034512461796

Received June 13, 2012; Last revision August 23, 2012; Accepted August 27, 2012

A supplemental appendix to this article is published electronically only at http://jdr.sagepub.com/supplemental.

Assessment of the Plasma/Serum IgG Test to Screen for Periodontitis

INTRODUCTION

Periodontitis is an infectious disease of the tissues surrounding the teeth and is a well-known silent infectious disease worldwide. It was reported that 50% of the population has bleeding gums, and the incidence rate of periodontitis is 35% in the USA (Albandar, 2002). According to recent studies, chronic periodontitis (persistent low-grade infection of periodontal pockets by Gram-negative bacteria) is associated with increased atherosclerosis, heart disease, diabetes mellitus, and other systemic diseases (Beck *et al.*, 2005; Michalowicz *et al.*, 2006; Tonetti *et al.*, 2007). Poor oral health may have a profound effect on general health. Therefore, efficient screening of periodontitis patients is essential for the maintenance of general health.

Generally, diagnosis of periodontitis is made by the examination of the periodontal condition, such as the prevalence of periodontal pockets, mobility of teeth, degree of tooth loss (Hefti, 1997), and behavioral factors such as smoking (Ryder, 2007). Since periodontitis is a polymicrobial infectious disease (Walker and Sedlacek, 2007), it is recognized that infection with periodontal bacteria leads to humoral immunological responses and elevates the serum IgG antibody levels against pathogens (Murayama *et al.*, 1988). Additionally, it has been reported that the serum IgG antibody titer against *Porphyromonas gingivalis* (*P. gingivalis*) decreased corresponding to the decrease in the bacterial count in periodontal pockets by periodontal treatment (Horibe *et al.*, 1995). Although the usefulness of the IgG antibody test for understanding periodontitis is recognized, this examination has not been widely adopted worldwide.

In this study, we first analyzed data from individuals with or without periodontitis, to evaluate the clinical usefulness of the blood IgG antibody titer test against periodontal pathogens for periodontitis screening, by determining the cut-off value of the titer using the receiver operating characteristic (ROC) curve. Second, the clinical usefulness of the IgG antibody test was evaluated in a nationwide clinical study on chronic periodontitis patients.

MATERIALS & METHODS

Study Design

An overview of the study is shown in Fig. 1. In cooperation with 11 university hospitals in Japan, 618 chronic periodontitis patients without systemic disease were registered between January 2007 and November 2009. From these, 536 patients (mean ages: 51.8 ± 13.9 yrs) were diagnosed according to the Guidelines of the American Academy of Periodontology (Krebs and Clem, 2006), and were enrolled in this study. At a company facility in Japan, 769 employees were

registered between September 2008 and November 2009. The oral conditions of 745 employees (mean age: 44.0 ± 9.1 yrs) were examined at work-related physical examinations, with the Community Periodontal Index (CPI; WHO, 1997). Of these, 629 employees with one of the following criteria (CPI of 1 to 4, gingivitis-positive, or over 40 yrs old) were excluded, and 116 employees were selected as the "Health" group (without periodontitis).

Pocket probing depth (PPD) was used as an index in oral examinations at university hospitals, while CPI was used at the company facility. Hence, it was not possible to unify the indices of periodontitis severity. To evaluate the effects of periodontal treatment, we examined periodontal conditions and IgG titers. The "Periodontitis" group was categorized by clinical parameters: ratio of gingival bleeding on probing (BOP) {the number of sites with BOP divided by the total number of sites *per* mouth (%): < 25, 25 – 50, > 50}; the score of periodontal lesions {the number of sites with periodontal lesions (PPD ≥ 4 mm) divided by the total number of sites *per* mouth (%): < 10, 10 – 30, > 30}. The severity of periodontitis was categorized into 2 groups by the presence or absence of sites of PPD over 4 mm, and the relation between periodontitis and blood IgG titer against *P. gingivalis* was analyzed with multiple cut-off values, which were set to 2×, 3×, 4×, and 5× on the basis of the cut-off value of IgG titer obtained in this study. Furthermore, 536 chronic periodontitis patients received periodontal treatment, including scaling and root planing (SRP), and instruction in proper home care techniques. Individual periodontal clinical parameters and IgG titers against periodontal pathogens for 312 chronic periodontitis patients were compared between 'before and after' periodontal treatment.

Informed consent was obtained from each participant, the protocol having been approved by the institutional review board at each institution.

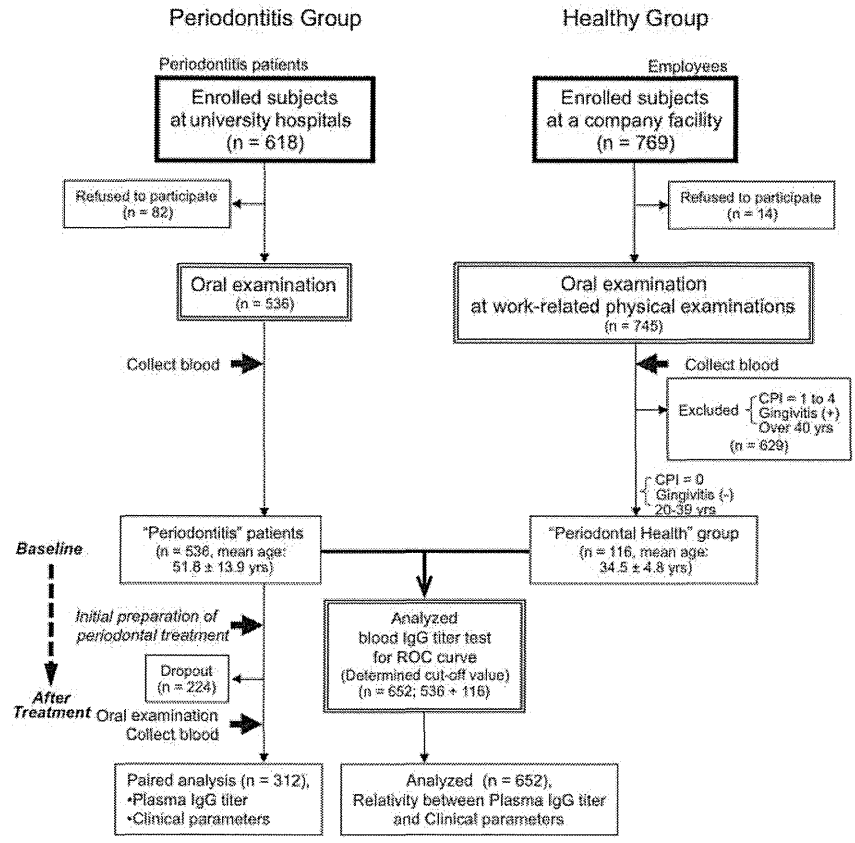

Figure 1. Flow chart of participant selection. Periodontal data were recorded by trained dental examiners at 11 university hospitals in Japan. The average number of periodontal lesions (PPD ≥ 4 mm), the score of BOP, and the score for mobile teeth were calculated for each patient. In contrast, in physical examinations at a company facility, the oral condition of employees was examined by assessment of CPI. Employees (CPI = 0, gingivitis-negative, and 20-39 yrs) were categorized as the "Periodontal Health" group for ROC curve analysis.

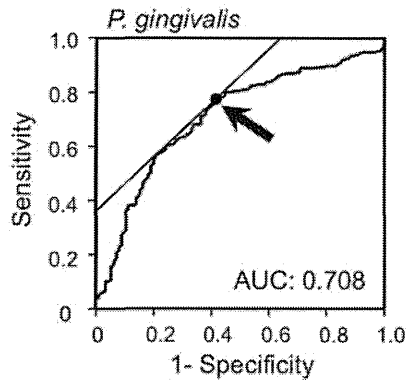

		Diagnostic test result		Total
		Periodontitis	Health	
plasma IgG Ab titer	>1.68	415	48	463
	<1.68	121	68	189
		536	116	652

Cut-off value	1.682
Sensitivity	0.774
Specificity	0.586

Figure 2. Setting cut-off value of the blood IgG antibody titer test against *P. gingivalis*. ROC curve of blood IgG antibody titer against *P. gingivalis* for the diagnosis of periodontitis. AUC, area under the curve.

Blood Sampling

In physical examinations at a company facility, serum samples were aliquoted and stored at -30°C. In university hospitals, the plasma from middle-finger fingertip capillary blood was obtained. From fingertip blood, a 50-μL quantity of whole blood was sampled, and device-treated plasma was obtained according to the procedures prescribed by Leisure, Inc. (Tokyo, Japan).

Measurement of IgG Titers against Periodontal Bacteria

Blood (serum or plasma) IgG antibody titers against periodontal pathogens were determined by Leisure with the enzyme-linked immunosorbent assay (ELISA) (Murayama *et al.*, 1988). As bacterial antigens, sonicated preparations of *P. gingivalis* FDC381, *Prevotella intermedia* (*P. intermedia*) ATCC25611, *Aggregatibacter actinomycetemcomitans* (*A. actinomycetemcomitans*) ATCC29523, and *Eikenella corrodens* (*E. corrodens*) FDC1073 were used. The sera from 10 healthy participants without periodontitis (ages 20-29 yrs) were pooled and used to calibrate the analyses. With serial dilutions of this pooled control serum, standard titration curves were prepared. The absorbance of each sample after reaction was defined as an ELISA unit (EU), so that 100 EU corresponds to 1:3,200 dilution of the calibrator sample (Appendix Table 1). According to the formula for clinical use, the mean ± 2 SD of the controls, based on the reported dataset of IgG titers to individual pathogens among 10 healthy individuals, was defined as 1 of the standard value.

Statistical Analysis

Statistical analysis was performed with JMP 9 (SAS Institute Inc., Cary, NC, USA). Wilcoxon's signed-rank test was used to evaluate individual treatment effects. The differences in levels of IgG against periodontal pathogens among each group with severity were analyzed by the Kruskal-Wallis and Steel-Dwass tests. The cut-off value of IgG titer was obtained from the ROC curve. Diagnostic efficacy evaluation was calculated and represented as sensitivity and specificity. The relation between periodontitis and IgG titer was analyzed by the Cochran-Mantel-Haenszel χ^2 test, adjusted for age, with categorization by cut-off value.

RESULTS

Screening Power of the IgG Titer Test for Periodontal Disease

Chronic periodontitis patients (n = 536) and periodontally healthy individuals (n = 116) were evaluated. Using ROC curves, we found that the area under the curve (AUC) of the IgG titers against *P. gingivalis* was the largest among those of other periodontal pathogens (*P. gingivalis*, 0.708; *A. actinomycetemcomitans*, 0.601; *E. corrodens*, 0.583; *P. intermedia*, 0.525). Therefore, we focused on *P. gingivalis* for further analysis, based on the literature (Fischer *et al.*, 2003; Akobeng, 2007) (Fig. 2). The optimal cut-off value for the test against *P. gingivalis* was 1.682. The sensitivity was 0.774, and the specificity was 0.586 at this value. We focused on *P. gingivalis* and *A. actinomycetemcomitans* for further analysis according to their AUC significance.

Change of IgG Titer in Response to Treatment

We examined the change of plasma IgG titer against *P. gingivalis* and *A. actinomycetemcomitans* with the initial preparation of periodontal treatment (n = 312 after treatment). Corresponding to the improvement of clinical parameters (% of PPD ≥ 4 mm, average of PPD, % of BOP, and % of mobile teeth were decreased: Fig. 3A) after intensive initial preparation, the plasma IgG titers against periodontal pathogens also decreased significantly (Fig. 3B).

IgG Titer and Severity of Periodontitis

We further evaluated whether the plasma IgG titer reflects the severity of periodontitis by combining data obtained from chronic periodontitis patients (n = 536) and periodontally healthy individuals (n = 116). The variances between categories (% of BOP and % of PPD ≥ 4mm) were analyzed. There were significant differences in the IgG titers against *A. actinomycetemcomitans* and *P. gingivalis* between BOP and PPD categories (Figs. 3C, 3D). In chronic periodontitis patients, IgG antibody titer to *A. actinomycetemcomitans* was significantly higher than that of healthy control individuals, but there was no significant increase for severity. In contrast, the titer to *P. gingivalis* increased significantly corresponding to the severity of periodontitis.

IgG Titer against *P. gingivalis* in Individuals with and without Sites of PPD ≥ 4 mm

Finally, we evaluated the relationship between the presence of sites of PPD ≥ 4mm (Table) and cut-off values of IgG titer against *P. gingivalis* by combining data obtained from chronic periodontitis patients and periodontally healthy individuals. IgG titers larger than each cut-off value were defined as positive. Individuals with and without sites of PPD ≥ 4 mm were more frequently associated with positive groups of IgG titer against *P. gingivalis* ($P < 0.0001$). Individuals with sites of PPD ≥ 4 mm were at least 3.54 times more likely to be positive (crude odds ratio at titer 3.36) in the IgG antibody test for periodontitis compared with those without sites of PPD ≥ 4 mm. When the cut-off value was raised, the sensitivity decreased and the specificity increased. At a cut-off value of 6.72, the sensitivity was 0.493 and the specificity was 0.810. Conversely, when the cut-off value was lowered to 1.0, the sensitivity increased to 0.828 and the specificity decreased to 0.490 (Table).

DISCUSSION

A method for the measurement of blood IgG antibody levels to periodontal pathogens has been developed for the diagnosis of periodontitis. However, this test has not been popularized in general dentistry. The reasons for this are likely as follows: (1) lack of standardized values for evaluating periodontitis, (2) psychological pressure associated with the taking of blood for both dentists and patients, and (3) lack of clinical recognition of the benefits. In this study, we used a commercial device for painless self-collecting of fingertip plasma from chronic periodontitis patients, instead of regular venous blood.

Based on the results of IgG titer against *P. gingivalis* in each participant, the ROC curve was drawn to determine the cut-off value. The AUC was moderately accurate for predicting

periodontitis. The optimal cut-off value for the test against *P. gingivalis* was 1.682. The sensitivity was satisfactory, whereas the specificity was low. The AUC for others tested showed low accuracy (below 0.700), suggesting that *P. gingivalis* is suitable for periodontitis screening. The age of the healthy control population in this study was set at 20 to 39 yrs. Thus, similar investigations among healthy people older than 40 yrs would be interesting for comparison.

Next, we examined whether the severity of periodontitis can be determined by this test, with *P. gingivalis* and *A. actinomycetemcomitans* selected according to their AUC accuracy (over 0.600). Clinical attachment level (CAL) has been more frequently used than PPD to evaluate the effect of periodontal treatment. However, even if teeth have high CAL, their PPD may be less than 3 mm. IgG titer levels must be influenced by the size of the area of infection, not by the history of tissue destruction. Therefore, we preferred PPD to CAL as a measure of periodontal severity. As expected based on previous reports (Alexander *et al.*, 1996; Behle *et al.*, 2009), the IgG titers against both bacteria were significantly decreased by periodontal treatment, corresponding to improvement in periodontal condition. The results suggested that this test is useful for evaluating treatment effects from the perspective of infection levels, and the test would be useful as a self-evaluation system for the effects of periodontal treatment. Furthermore, we found that the titer to *P. gingivalis*, not to *A. actinomycetemcomitans*, increased significantly corresponding to the severity of periodontitis. It has been reported that the correlation between the number of periodontal pockets and the antibody levels to *P. gingivalis* was stronger than that for *A. actinomycetemcomitans* (Pussinen *et al.*, 2011). These results are reasonable, since chronic periodontitis is caused mainly by obligate anaerobic bacteria, *P. gingivalis*.

Finally, the relation between periodontitis and the IgG titer against *P. gingivalis* was analyzed with multiple cut-off values. No account was taken of smoking or sex during this study. There

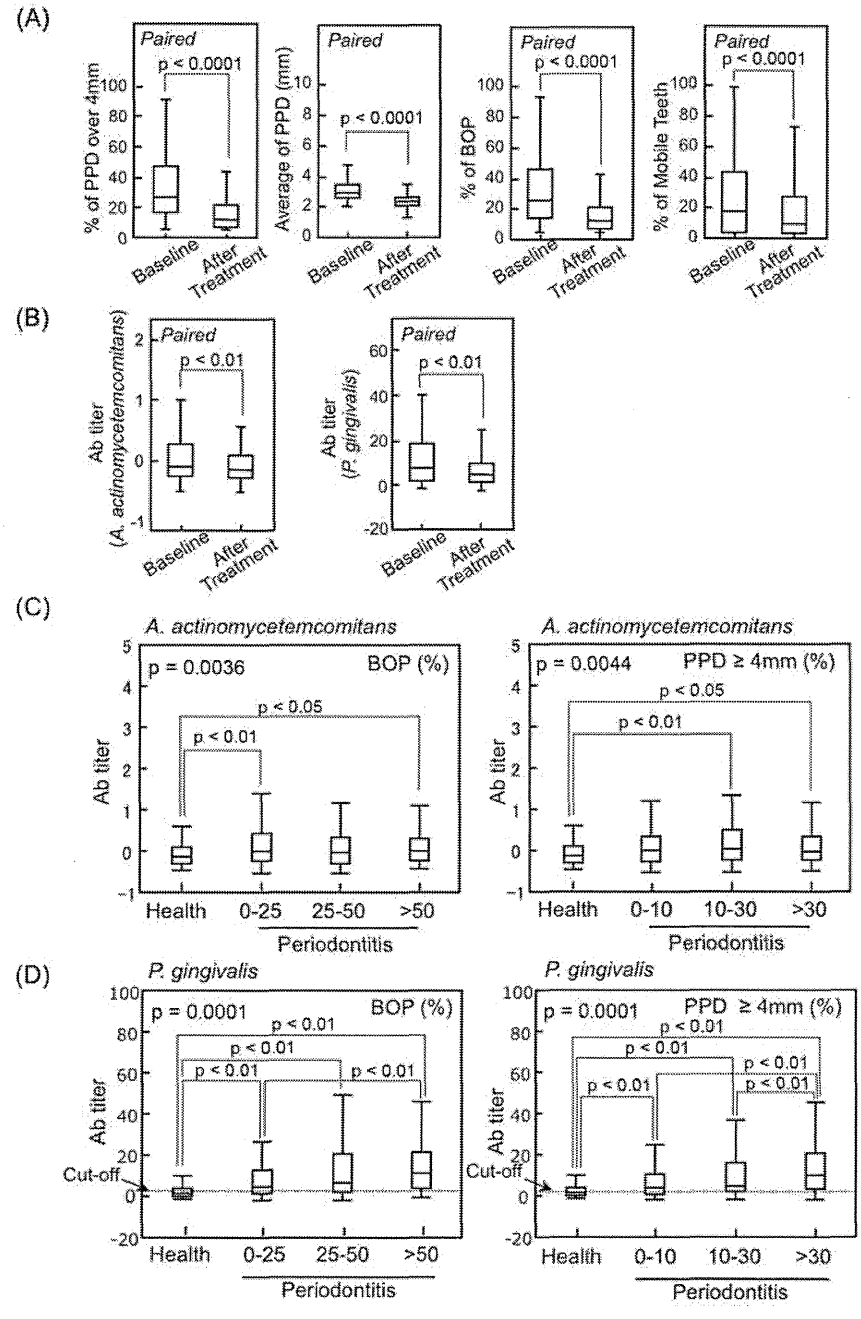

Figure 3. Blood IgG antibody levels reflecting periodontal treatment and severity of periodontitis. Individual periodontal clinical parameters **(A)** and plasma IgG antibody levels against periodontal pathogens **(B)** of 312 chronic periodontitis patients were compared between baseline and after intensive periodontal treatment. The periodontal clinical parameters are % of PPD ≥ 4 mm, average of PPD, % of BOP, and % of mobile teeth. The periodontal pathogens were *A. actinomycetemcomitans* and *P. gingivalis*. These data were analyzed by Wilcoxon's signed-rank test for paired samples. Box plot shows median, the lower and upper quartiles, and the minimum and maximum of all the data. Plasma IgG antibody levels against *A. actinomycetemcomitans* **(C)** and *P. gingivalis* **(D)** were compared among categorized groups (% of BOP, Healthy: n = 116, 0-25: n = 307, 25-50: n = 124, > 50: n = 105; % of PPD ≥ 4 mm, Healthy: n = 116, 0-10: n = 154, 10-30: n = 186, > 30: n = 196). These data were analyzed by the Kruskal-Wallis test for overall group differences and the Steel-Dwass test for between-group differences. Cut-off, IgG titer = 1.86 for *P. gingivalis*.

Table. Relation between Pocket Depth and Cut-off Value of Blood IgG Antibody Level against *P. gingivalis*

	Titer	1.00		1.68		3.36		5.04		6.72		8.40	
Cut-off value of IgG titer	n/p (%)	n 24	p 76	n 29	p 71	n 41	p 59	n 51	p 49	n 58	p 42	n 62	p 38
Sites of PPD ≥ 4 mm (n = 652)	Absence (%)	11	12	13	10	15	8	17	5	19	4	19	4
	Presence (%)	13	64	16	61	26	51	34	44	39	38	43	34
Statistical analysis	Sensitivity	0.828		0.790		0.659		0.560		0.493		0.440	
	Specificity	0.490		0.565		0.646		0.769		0.810		0.837	
	Crude OR	4.61		4.48		3.54		4.24		4.13		4.02	
	95%CI	3.10 – 6.86		3.30 – 7.21		2.41 – 5.20		2.78 – 6.46		2.64 – 6.46		2.51 – 6.44	
	p value	< 0.0001		< 0.0001		< 0.0001		< 0.0001		< 0.0001		< 0.0001	

The numbers of negative and positive (n/p) individuals were converted to percentages. Severity of periodontitis was categorized into 2 groups based on the presence or absence of sites of PPD ≥ 4 mm, and numbers of participants were converted to percentages. Total number of participants = 652. Because percentage was rounded off, sample number of "sites of PPD ≥ 4 mm" was different from a real number (n = 147). Statistical comparisons of the categorical variables were conducted by the Cochran-Mantel-Haenszel χ^2 test adjusted for age. Crude OR, Crude odds ratio; 95%CI, 95% confidence interval; *p < 0.0001.

were significantly more females than males in this study (Appendix Table 2). At the university hospitals, female outpatients were usually more common than males. Additionally, females may be more health-conscious than males. Nonetheless, analysis of our data indicated that the crude ORs were high, at more than 3.54. Notably, the more severe the periodontitis, the higher the crude OR. Some suggest that odds ratios greater than 4 in case-control studies provide strong support for causation (Grimes and Schulz, 2002). Accordingly, these results indicate the possibility that the IgG titer against *P. gingivalis* is associated with periodontal severity. From investigation of adults aged over 40 yrs in parsimonious models including demographic data, smoking, and diagnosed diabetes, Dye *et al.* (2009) showed that high IgG titers to *P. gingivalis* were most strongly associated with periodontitis across all definitions (OR, 2.07 to 2.74) in unadjusted models. Future investigation controlling these factors may provide greater insights into this relationship.

Screening the chronic periodontitis patients with the various cut-off titers of this test may be able to detect those patients highly sensitized with *P. gingivalis*. This offers a clear advantage in selecting periodontitis patients at risk for lifestyle-related diseases associated with periodontitis. In contrast, there is a disadvantage in filtering out periodontitis patients less sensitized with *P. gingivalis* but with clinical symptoms. They may refrain from visiting the dental clinic, and therefore the periodontitis would remain untreated. To prevent this, it is important for screening tests to increase the sensitivity by reducing the cut-off value, assuming a decrease in specificity. Consequently, we consider that a cut-off value of 1.0 is the most suitable for screening. IgG titer reflects the existence of host immune-response against pathogens, thus showing the history of infection. Since response is delayed by the infection, sometimes the pathogen itself is not detected. There is a report describing the presence of *P. gingivalis* as the strongest determinant of the systemic antibody response to these pathogens, and contending that the extent of periodontitis has, at most, a modest modifying effect (Pussinen *et al.*, 2011). The practical use of this IgG titer test may lead to early detection of chronic periodontitis. In addition, caution must be taken for periodontal patients with unusual immune-responses, such as aggressive forms of periodontitis. Further studies are needed for expanded indications.

In conclusion, the results of this study supported the blood IgG antibody titer test as useful for the screening of latent periodontitis patients with high IgG titers to periodontal pathogens without subjective symptoms (Ohyama *et al.*, 2001), and for the prognostication of periodontitis recurrence in individuals without symptoms during supportive periodontal therapy (Sugi *et al.*, 2011). In addition, chronic low-grade inflammation is believed to have an effect on long-term health and on chronic lifestyle-related diseases. Thus, it is important to establish a test system for efficient evaluation of periodontal infection for physicians. It is possible to send plasma samples to a clinical laboratory by regular mail or courier. Therefore, it would be convenient for users if an online system for ordering the kit and retrieving test results could be established. This system facilitates periodontal examination for people with no time to visit a dental clinic.

ACKNOWLEDGMENTS

This study was supported by a Grant-in-Aid for Scientific Research (A) (No. 18209061) from the Japan Society for the Promotion of Science and by a Health Labor Sciences Research Grant (Comprehensive Research on Aging and Health, H19-Choju-008) from the Ministry of Health, Labor, and Welfare of Japan. The authors declare no potential conflicts of interest with respect to the authorship and/or publication of this article.

REFERENCES

Akobeng AK (2007). Understanding diagnostic tests 3: Receiver operating characteristic curves. *Acta Paediatr* 96:644-647.

Albandar JM (2002). Periodontal diseases in North America. *Periodontol* 2000 29:31-69.

Alexander DC, Martin JC, King PJ, Powell JR, Caves J, Cohen ME (1996). Interleukin-1 beta, prostaglandin E2, and immunoglobulin G subclasses